

Water Resources Research®

RESEARCH ARTICLE

10.1029/2024WR037726

Carly H. Hansen and Bilal Iftikhar share first-authorship.

Key Points:

- Estimates of total surface area and littoral area of US reservoirs vary three-to four-fold depending on the source of data and depth threshold used to delineate littoral area
- Relative to their maximum extent, the area of larger and hydroelectric reservoirs fluctuates less than small and nonhydroelectric reservoirs; interannual and seasonal recurrence of water is also more consistent in large reservoirs
- Estimates of reservoir GHG emissions based on field-measured methane and carbon dioxide should account for fluctuations in lake levels and surface area

Supporting Information:

Supporting Information may be found in the online version of this article.

Correspondence to:

C. H. Hansen,
hansench@ornl.gov

Citation:

Hansen, C. H., Iftikhar, B., Pilla, R. M., Griffiths, N. A., Matson, P. G., & Jager, H. I. (2025). Temporal variability in reservoir surface area is an important source of uncertainty in GHG emission estimates. *Water Resources Research*, 61, e2024WR037726. <https://doi.org/10.1029/2024WR037726>

Received 17 MAY 2024

Accepted 26 NOV 2024

Author Contributions:


Conceptualization: Natalie A. Griffiths, Paul G. Matson, Henriette I. Jager

Formal analysis: Bilal Iftikhar, Rachel M. Pilla

Methodology: Bilal Iftikhar

© 2025 Oak Ridge National Laboratory. This is an open access article under the terms of the [Creative Commons Attribution-NonCommercial-NoDerivs License](#), which permits use and distribution in any medium, provided the original work is properly cited, the use is non-commercial and no modifications or adaptations are made.

Temporal Variability in Reservoir Surface Area Is an Important Source of Uncertainty in GHG Emission Estimates

Carly H. Hansen¹ , Bilal Iftikhar², Rachel M. Pilla¹, Natalie A. Griffiths¹ , Paul G. Matson¹, and Henriette I. Jager¹

¹Environmental Sciences Division, Oak Ridge National Laboratory, Oak Ridge, TN, USA, ²Irrigation Department, Government of Punjab, Islamabad, Pakistan

Abstract Ebullitive methane (CH₄) emissions in lentic ecosystems tend to concentrate at river-lake interfaces and within shallow littoral zones. However, inconsistent definitions of the littoral zone and static representations of the lake or reservoir surface area contribute to major uncertainties in greenhouse gas (GHG) emissions estimates, particularly in reservoirs with large water-level fluctuations. This study examines temporal variation in littoral and total surface areas of US reservoirs and demonstrates how different methods and data sources lead to discrepancies in reservoir GHG emissions at large scales and over time. We also explore variability in remotely sensed water occurrence according to maximum surface area, reservoir purposes, and hydrologic regions. Notably, the largest relative variability in surface area is exhibited by small reservoirs with a maximum surface area <1 km² and non-hydroelectric reservoirs. Additionally, we use a case study of measured CH₄ emissions from the southeastern United States (Douglas Reservoir) to illustrate the effects of varying surface area on reservoir-wide GHG estimates. Upscaled CH₄ emissions in Douglas Reservoir differed by nearly two-fold depending on the source of total surface area data and whether estimates accounted for seasonal fluctuations in surface area. During seasonal drawdown in Douglas Reservoir, relative littoral area varies non-linearly; periods of lower pool elevation (and thus larger relative littoral area) likely contribute disproportionately high CH₄ emission rates compared to the commonly sampled summer season when water levels are at full-pool elevation. Improved GHG monitoring and upscaling techniques require accounting for temporal variability in reservoir surface extent and littoral area.

Plain Language Summary Reservoirs can emit methane through several pathways, including bubbling from sediments which occurs most often in shallow zones. Different methods for estimating the area of this zone and disagreements in waterbody data sets results in uncertainty for large-scale estimates of waterbody characteristics and methane emissions. Water detection algorithms applied to historical satellite imagery show that smaller reservoirs and those used for non-hydroelectric purposes tend to have the highest variability in relative surface area. The high seasonal variability in both surface area and measured methane emissions, which contributes to uncertainty in the overall reservoir GHG footprint, is illustrated using data collected from Douglas Reservoir, in East Tennessee, USA.

1. Introduction

Surface area is often used in both estimating and comparing greenhouse gas (GHG) emissions from waterbodies (Bastviken et al., 2004; Rosentreter et al., 2021; Scherer & Pfister, 2016), but there are major uncertainties and limitations in how it is applied to individual and large-scale GHG accounting cases. Lake and reservoir surface area has been evaluated at the global scale, largely thanks to satellite imagery that can accurately distinguish surface water extent and track changes over time (Bonnema et al., 2022; Keller et al., 2021; Pekel et al., 2016). Global waterbody surface area estimates vary widely; total lake and reservoir area ranges from 2.67 to 5.36 million km² because of differences in water-detection algorithms, spatial resolutions used to delineate surface area, size thresholds used to identify waterbodies, and assumed distributions of size used for extrapolation (Downing et al., 2006; Messenger et al., 2016; Verpoorter et al., 2014). Additionally, surface area is temporally dynamic, especially in reservoirs where storage and releases can be highly regulated (Bonnema et al., 2022; Yizgaw et al., 2018).

Project administration: Natalie A. Griffiths
Visualization: Bilal Iftikhar, Rachel M. Pilla
Writing – original draft: Bilal Iftikhar, Rachel M. Pilla, Henriette I. Jager
Writing – review & editing: Rachel M. Pilla, Natalie A. Griffiths, Paul G. Matson, Henriette I. Jager

Regional and global waterbody inventories lack key details about the context of reported values, such as the elevation at full pool. Does the surface area reported reflect the designed maximum extent, or the historical average in inundated area, or its seasonal drawdown (e.g., flood mitigation or supply)? The National Inventory of Dams (NID) for the United States (US) synthesizes reports from various owners and regional agencies and describes surface area as the “size of the impoundment at a normal retention level” (USACE, 2023); however, “normal” operating conditions generally allow a range of elevations during high- or low-flow periods. On the other hand, reported surface areas and waterbody boundaries in HydroLAKES (Messenger et al., 2016) were largely derived from a digital elevation model without any context about reservoir stage or surface area. Studies that use surface area as a predictive variable in statistical models of reservoir GHG footprints (Bastviken et al., 2004; Scherer & Pfister, 2016) do not account for temporal variation in water levels (surface area) or the impact of fluctuating water levels on GHG measurements used to develop empirical relationships.

Waterbody surface area is also key to describing the littoral zone, which has been defined as the transitional zone of the bottom of a lake or reservoir (as opposed to the open water) that supports macrophyte growth (Wetzel, 2001). More specifically, it is the area where enough light can penetrate to the bottom of the lake to support photosynthesis, regardless of actual macrophyte presence (Seekell et al., 2021). The littoral zone is often used as a proxy for the area where CH₄ ebullition occurs (Shi et al., 2021). This is because the shallow water depths correspond with low hydrostatic pressure which allows CH₄ bubbles to be released from the sediment with little opportunity for oxidation before reaching the water surface. Contributions of CH₄ ebullition can range from 0 to almost 100% of the measured whole-lake CH₄ flux (Deemer et al., 2016). While ebullition has been detected from open water sites as deep as 30 m, the majority of CH₄ ebullition occurs in shallower areas often designated as the littoral area (Beaulieu et al., 2016) or zones with emergent vegetation (Kyzivat et al., 2022).

The lack of consistency in defining the littoral zone adds to the challenges in GHG accounting given the variety of factors that contribute to GHG production and emissions. Littoral area is sometimes defined with reference to a depth threshold, but the threshold differs among studies (Table 1). In other cases, littoral area is defined relative to surface area (i.e., as a percentage of the total surface area of the waterbody). In the absence of detailed in-situ bathymetric, macrophyte, and/or light penetration data, the littoral area is often approximated from easily obtainable morphometric characteristics, such as reservoir size, depth, and shoreline complexity. Empirical relationships between littoral area and these characteristics vary in how well they have been validated and the degree to which they generalize to unsampled waterbodies (Seekell et al., 2021).

None of the methods used to define the littoral area account for variability in total surface area due to reservoir withdrawals, releases, variable inflows, or groundwater seepage and evaporative losses. Failure to account for seasonal fluctuations in reservoir water levels and associated changes in partitioning of littoral and surface area could have major implications for CH₄ emissions either directly (i.e., by altering hydrostatic pressure and changing the area and oxidative state of the littoral zone) or indirectly (that is, by influencing water quality and algal productivity; (Cantonati & Lowe, 2014; Geraldes & Boavida, 2005)).

Understanding estimates of surface area and littoral area and their dynamics is crucial because they are often used either to upscale emissions or as a proxy for emissions under the assumption that carbon dioxide (CO₂) diffusion occurs in the pelagic zone and CH₄ ebullition occurs in the littoral zone. In a study of large global reservoirs using the G-res model (a GHG emissions model for reservoirs), a 10% increase in the global littoral area increased the estimated annual total GHG flux (CO₂ and CH₄) by more than 190% (Harrison et al., 2021). When the littoral zone is completely exposed during reservoir drawdown, this could result in a dramatic shift in emissions and dominant pathways for carbon, increasing CO₂ emissions and decreasing CH₄ emissions because dry sediment is typically dominated by CO₂ rather than CH₄ emissions (Keller et al., 2021).

In this study, we compare estimates of reservoir littoral area and surface area obtained from remotely sensed data products and bathymetry data sets for the US. We examine variability in these estimates at both regional (cumulative) and individual waterbody scales (distributions of waterbodies). We also examined whether there were differences in variability surface area within a reservoir based on maximum surface area, primary purposes, and hydrologic region. Additionally, we evaluate the variability in waterbody extent and concurrently measured GHG emissions in Douglas Reservoir in East Tennessee, USA, and used this case study to demonstrate how changes in surface area and littoral area can be accounted for in reservoir-wide GHG emissions estimates. The wide ranges we observe in water surface area, littoral area, and estimates of GHG emissions derived from them underscore

Table 1

Comparison of Methods to Estimate Littoral Area and Suggested Relationships Between Littoral Area and Other Lake Characteristics

Relationships between littoral area and other lake characteristics	Strengths and limitations
Inverse relationship between littoral area (relative to total surface area) and the mean depth (Henson, 1993)	Simple, using characteristics that are supported by widely available data. Henson (1993) assumes a 4 m depth threshold for the littoral area but acknowledges littoral area may be between 0 and 10 m; does not reflect variability in surface area or depth. Others suggest the littoral zone depth is between 1 and 5 m (Zohary & Gasith, 2014).
Littoral zone is estimated from the shoreline development index (ratio of shore length to the circumference of a circle with the same area as the lake) (Wetzel, 2001)	Simple, using characteristics that are widely available Empirical evidence does not consistently support the assumption that lakes with more convoluted shorelines will have larger littoral zones (Seekell et al., 2021)
Littoral zone is designated as the area that is 10 m from the shoreline, not accounting for depth (USEPA, 2007)	Methodology can be easily replicated for large-scale sampling, requiring minimal equipment, which makes it ideal for surveys such as the National Lakes Assessment
Littoral area is estimated as a percentage of the total surface area using the relationship between maximum and mean depth and an assumed threshold (Equations 1 and 2)	Simple, using widely available characteristics Assumes a 3 m depth threshold for littoral area; does not reflect variability in surface area or depth
Littoral habitat size is based on empirical hypsometric relationships such as the mean-to-maximum depth ratio (Seekell et al., 2021)	Developed and validated for natural lakes but is expected to apply to reservoirs. Requires information about light penetration (e.g., water clarity)

why accounting for surface area and littoral dynamics is critical to reducing uncertainty in carbon accounting for reservoirs.

2. Data and Methods

2.1. Data Acquisition

Reservoir geometry data for US reservoirs were obtained from the HydroLAKES data set ($n = 1,891$ reservoirs in the US), which describes basic geometric information about global lakes and reservoirs with $>0.1 \text{ km}^2$ area (Messenger et al., 2016). HydroLAKES is also the foundation of GLOBathy (Khazaei et al., 2022), modeled bathymetric data in raster form that includes estimates of maximum reservoir depth based on the individual morphological characteristics of the reservoir. Bathymetric contours were calculated for GLOBathy rasters at 1 m intervals for each reservoir using the *sf* and *terra* packages in R (Hijmans et al., 2022; Pebesma, 2018; R Core Team, 2023). Reservoir data (surface area, purposes) were also retrieved from the NID (USACE, 2023), and limited to waterbodies with non-zero values reported for both storage and surface area ($n = 65,907$).

Links between reservoirs from HydroLAKES and hydroelectric infrastructure were established using two data sets: the Global Reservoir and Dams database (GRanD) (Lehner et al., 2011) and the Hydropower Infrastructure—Lakes, Reservoirs, and Rivers (HILARRI) data set (Hansen & Matson, 2022). The HILARRI data set connects all operational hydroelectric facilities (dams and power plants) in the US and Puerto Rico with their associated waterbodies (lakes, reservoirs, or rivers). This enabled the classification of reservoirs based on purpose and determine whether each reservoir is associated with hydroelectric generation as either the primary purpose or a secondary purpose (i.e., operations are primarily for flood control, water supply, or another purpose other than hydroelectric). A distinction between whether hydroelectric is the primary versus secondary purpose is made to further explore which objectives are associated with greater variability in reservoir surface area or littoral area estimates. Additionally, hydrologic regions (2-digit hydrologic unit codes [HUC-2] (USGS, 2014)) were used to summarize data by geographic regions of the US.

Water occurrence, water recurrence, and maximum surface water extent were extracted from the Global Surface Water (GSW) data set (Pekel et al., 2016), a Landsat-based global remote-sensing record of surface water at 30-m resolution that extends from 1984 to 2021. The GSW-calculated water occurrence describes the percent of the time during the 38-year period of record when water was detected in a given pixel. GSW recurrence is measured seasonally, describing the number of months where water is detected, as well as on an interannual basis, describing the frequency with which water returns from year to year at each pixel, that is, the interannual behavior of water occurrence in water bodies. In the GSW data set, the recurrence value was calculated on a pixel-by-pixel basis in two steps: (a) determine which months water had been detected, that is, the “water season,” and (b)

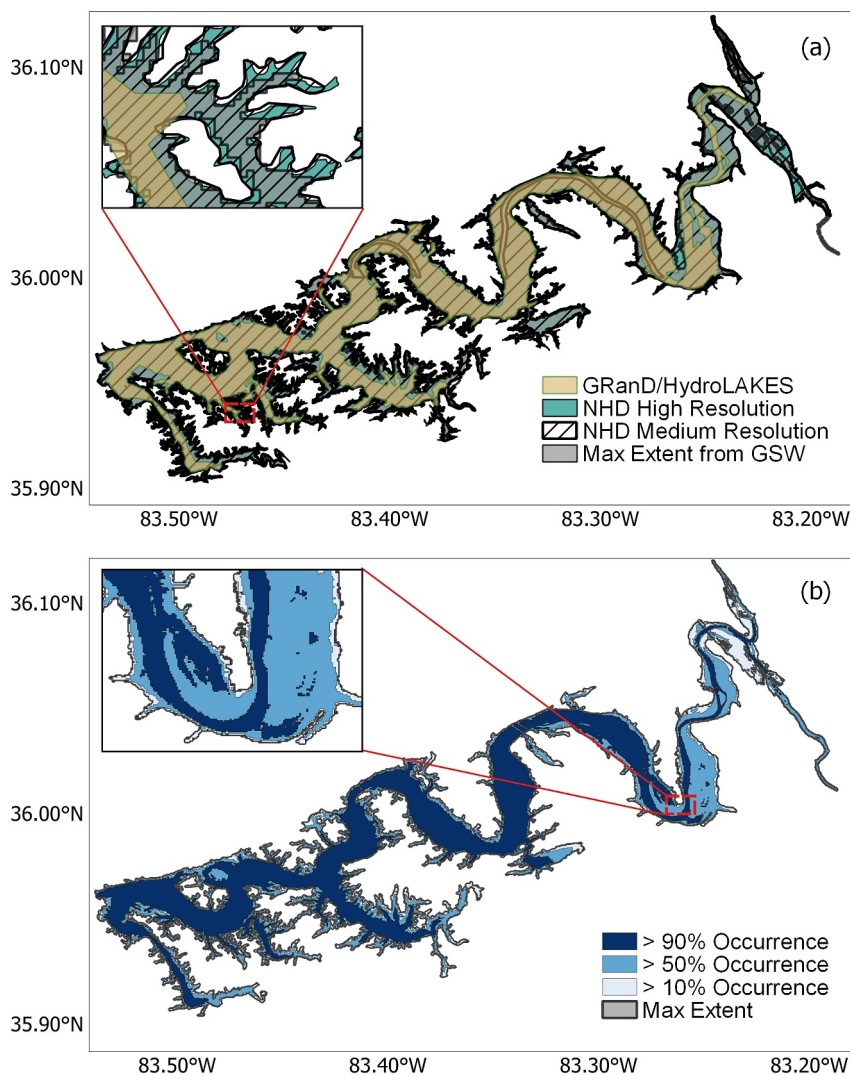


Figure 1. Illustration of different surface areas of Douglas Reservoir, USA according to (a) polygons included in various national and global data sets and (b) water-occurrence thresholds from the Global Surface Water data set. In panel (a), note the differences in detail near the reservoir perimeter between medium and high-resolution NHD data sets (see inset). In panel (b), the dark blue area shows where pixels were classified as water for at least 90% of the Landsat record (1984–2021) whereas the medium blue and light blue areas are associated with pixels classified as water for at least 50% and 10% of the record, respectively. The maximum extent of the reservoir (pixels classified as water at least once during the record) is shown as a black outline.

determine the fraction of years in the satellite record when water was detected during the water season (Pekel et al., 2016).

Each image in the GSW image collection was clipped according to the boundary of the HydroLAKES polygon, which we assumed is a bounding extent for each waterbody in the national-scale analysis. We compared remotely sensed maximum water extent, the HydroLAKES polygon, and boundaries obtained from other sources (National Hydrography Data set (NHD) (USGS, 2018), National Hydrography Data set Plus High Resolution (NHD + HR) (USGS, 2021)) (Figure 1a). Although the actual surface water may extend beyond the bounds of the HydroLAKES polygon, we assumed that HydroLAKES boundaries describe the maximum extent. This is because it was not possible to distinguish individual waterbodies accurately and systematically from GSW satellite imagery (i.e., to ensure no adjacent waterbodies were included and defining where the river ends, and the reservoir begins). Forcing water occurrence to conform to the HydroLAKES outline allowed us to maintain consistent comparisons of surface area, littoral area, and water detection statistics. The maximum water extent for each reservoir was

calculated from pixels within the HydroLAKES boundary where water was detected at least once during the 38-year Landsat record.

2.2. Derived Metrics for Analysis of Variability in Surface and Littoral Areas

Three metrics of surface area (SA) were calculated using data from different sources: surface area according to HydroLAKES (SA_H), surface area reported in the NID (SA_{NID}), and maximum surface water extent within the HydroLAKES boundary according to the GSW data set (SA_{GSW}). We also calculated the surface water area for various percentile thresholds of water occurrence (10%–90%) using the GSW data set, SA_x , where x is the threshold percentile of surface water occurrence. We calculated the relative area by dividing the area at a given water occurrence threshold, SA_x , by SA_{GSW} to facilitate comparisons between large and small reservoirs (maximum surface area $<1 \text{ km}^2$). Relative surface area (% of maximum extent detected as water) across water occurrence thresholds provides a useful description of long-term historical reservoir variability. For example, a reservoir with relative surface area of 50% at a water occurrence threshold of 80% would indicate that only 50% of pixels were identified as water in at least 80% of the Landsat record (1984–2021). A steep decline in relative surface area as the water occurrence threshold increases suggests a history of large fluctuations in reservoir surface area. Reservoirs with large differences ($>5\%$) between GSW max extent and the reported surface area in HydroLAKES were excluded from our analyses. This reduced our sample size for assessing surface area fluctuations to 1,399 reservoirs, 75% of the original data set considered for this study.

We illustrate these definitions for Douglas Reservoir in East Tennessee, USA. An example of how different reservoir areas correspond with the maximum extent and 10% (i.e., water present in a pixel 10% of the time), 50% (water present in a pixel half of the time), and 90% (water present in a pixel 90% of the time) occurrence thresholds for is shown in Figure 1b.

We compared median and IQR of relative surface area by reservoir purpose (obtained from either the NID or GRanD databases) across different thresholds of water occurrence. Additionally, we obtained local climate and topographical characteristics of each reservoir, including average annual runoff (mm yr^{-1}) and surface-level air temperature ($^{\circ}\text{C}$) between 1984 and 2021 from TerraClimate (Abatzoglou et al., 2018) and elevation (m) from the Global Multi-resolution Terrain Elevation Data set (Danielson & Gesch, 2011). Pearson correlations were calculated for each of these variables to explore their relationships with surface area variability (measured as relative surface area across different water occurrence thresholds).

Littoral area (LA) was calculated using one of two different methods. First, we used the equations from the G-res model (LA_{G-res} ; Equations 1 and 2 (Prairie et al., 2017)).

$$\% \text{ LA} = \left(1 - \left(1 - \frac{3}{\text{Max Depth}} \right)^q \right) * 100 \quad (1)$$

$$q = \frac{\text{Max Depth}}{\text{Mean Depth}} - 1 \quad (2)$$

Additional estimates were obtained from bathymetric contours (LA_{Bath}), assuming 3-m, 4-m, and 10-m depth thresholds. We reported the number of reservoirs with acceptable (positive) littoral areas in the summaries (Table 2). Note that, in some cases, the information provided by HydroLAKES or GLOBathy was insufficient or wrong, leading to negative littoral areas. For instance, for some reservoirs, the reported reservoir depth (from HydroLAKES) exceeded the maximum depth (modeled depth from GLOBathy). For these reservoirs, LA_{G-res} was not calculated, and these reservoirs were not included in comparisons of the distribution or sum of littoral area. In other cases, the minimum depth of the modeled bathymetry exceeded the threshold used to define the littoral area. For reservoirs where the maximum depth was less than the specified littoral-area threshold (i.e., 3-m, 4-m, or 10-m), the littoral area was assumed to be equal to the entire surface area of the reservoir, as outlined by HydroLAKES/GLOBathy.

We used non-parametric Wilcoxon signed-rank tests to evaluate whether estimates of SA were significantly different between values reported in HydroLAKES (SA_H) and the NID (SA_{NID}), and the SA_H and the maximum extent detected by the GSW data set (SA_{GSW}). These tests were also used to compare estimates of LA at each depth threshold (e.g., $LA_{Bath-3m}$ and $LA_{G-res-3m}$). The Kruskal-Wallis One-Way Analysis of Variance (ANOVA)

Table 2
Comparison of Calculated Surface Area (SA), Littoral Area (LA), and Estimated Total Annual CH₄ Flux for US Reservoirs According to Different Data Sources and Methods

Metric	n	Area (km ²)				Estimated methane (Tg CH ₄ yr ⁻¹)
		Cumulative	Mean	Median	Standard deviation, σ	
<i>Surface Area</i>						
SA _H	1,891	37,758	19.97	4.91	64.88	0.64
SA _{GSW}	1,891	36,716	19.42	4.75	63.95	0.62
SA _{NID}	65,912	176,411	2.68	0.05	319.95	2.94
<i>Littoral Area</i>						
LA _{G-res-3m}	1,152	7,302	6.34	1.06	23.85	–
LA _{Bath-3m}	1,590	6,048	3.80	1.15	17.28	–
LA _{G-res-4m}	1,156	9,076	7.85	1.43	29.07	–
LA _{Bath-4m}	1,681	8,836	5.26	1.58	21.57	–
LA _{G-res-10m}	1,256	16,853	13.42	3.17	46.84	–
LA _{Bath-10m}	1,842	21,608	11.73	3.56	38.94	–

Note. Subscripts for surface area include H = HydroLAKES, GSW = Maximum extent from GSW data set limited to the HydroLAKES boundary, NID = National Inventory of Dams. Subscripts for littoral area include G-res-Xm = G-res formula and Bath-Xm = GLOBathy bathymetric data, limited by a depth threshold of X meters. Estimates of CH₄ ebullition and diffusion for LA_{G-res} and LA_{Bath} areas are not included because existing models require other inputs in addition to the littoral area.

test was also used to evaluate variations in relative littoral area (LA) among groups categorized by primary reservoir purpose and region. Finally, we used the different estimates of reservoir surface area and published estimates of CH₄ emissions to demonstrate how differences in reservoir surface area affect upscaled GHG emission estimates at the national scale. (Rosentreter et al., 2021) calculated median areal flux for two classes of reservoir size: 26.1 mg CH₄ m⁻² d⁻¹ for reservoirs with surface area <1 km² and 46.4 mg CH₄ m⁻² d⁻¹ for reservoirs with >1 km². These median CH₄ values were multiplied by the total area in each size class according to SA_H, SA_{GSW}, and SA_{NID}. The values were then summed across the data sets and multiplied to obtain an estimate of annual CH₄ flux reservoirs in the US.

2.3. Case Study – Douglas Reservoir

Douglas Dam on the French Broad River in East Tennessee, USA, was constructed in 1942, mainly for hydroelectric generation and flood control. Douglas Reservoir is a warm, monomictic reservoir with a water residence time of approximately 3 months. The reservoir drains a mountainous 11,738 km² watershed that is composed of developed areas, croplands, rangelands, and forests. The Tennessee Valley Authority (TVA) operates the reservoir and associated powerhouse as a peaking plant, increasing the discharge for a few hours each day to near the full capacity of one or more of the turbines to provide electricity during the peak demand periods of each day and week (net capacity is 182 MW during the summer). While GHG emissions at Douglas Reservoir have not been historically measured, water quality has been regularly evaluated over the past two decades; it fluctuates between a “poor” and “fair” rating for ecological health, primarily due to low dissolved oxygen and high chlorophyll (TVA, 2023).

Douglas Reservoir was sampled for CH₄ emissions during different levels of drawdown in December 2021 April 2022, and October 2022 (Pilla et al., 2023). Methods followed those presented in (Bevelhimer et al., 2016) across six stations (three cove and three main channel) for measurements of CH₄ surface diffusion, ebullitive emissions, and degassing emissions. In brief, CH₄ diffusive surface emissions were measured using a floating surface chamber connected to a Los Gatos Research Microportable Gas Analyzer (918 series). Gas concentrations in the chamber headspace were recorded at one-second intervals for at least two continuous minutes, and diffusive emissions were calculated according to Equation 1 in (Bevelhimer et al., 2016). CH₄ ebullitive emissions were measured using inverted passive funnel traps that were deployed over one to two nights. Gas collected in the

funnel traps were processed in the laboratory on a Shimadzu Gas Chromatograph (GC-2014) following standard gas chromatography procedures. CH₄ ebullitive emissions were calculated according to Equation 2 in (Bevelhimer et al., 2016). CH₄ degassing emissions were measured as the difference in dissolved gas concentration between the forebay and tailwater, using the headspace-analysis method and processing samples on a Shimadzu Gas Chromatograph (GC-2014), multiplied by daily discharge.

To evaluate uncertainty in upscaled CH₄ emission estimates arising from different waterbody data sources, we compared estimates of reservoir surface area across the following data sources: GRanD (Lehner et al., 2011), HydroLAKES (Messenger et al., 2016), National Hydrography Data set (NHD) (USGS, 2018), National Hydrography Data set Plus High Resolution (NHD + HR) (USGS, 2021), and the NID (USACE, 2023). The surface area estimates were assumed to be at full pool and then adjusted using empirical bathymetry data and drawdown levels corresponding to each sampling date (11.3 m drawdown in December 2021, full pool in April 2022, and 3.7 m drawdown in October 2022). Hypsographic curves relating surface area and depth were developed by manually digitizing fishing map contours at five depths, plus the total surface area from each shapefile data source. The best-fit polynomial curve (highest R^2) for the hypsographic data from each data source was selected and then used to estimate littoral area (depth <3 m) at different pool elevations for each data source (Figure S1 in Supporting Information S1).

Diffusive and ebullitive fluxes were upscaled to the whole reservoir based on weighted averaging of the cove versus main channel sites as described in (Bevelhimer et al., 2016). Here, the upscaled fluxes were calculated using Equation 3,

$$\text{Whole reservoir flux} = SA \times \sum_{i=1}^n p_i \times \bar{F}_i \quad (3)$$

where SA is the surface area, p is the proportion of surface area considered cove or main channel (41% and 59%, respectively), and F is the mean flux across the three sites in the cove or main channel areas. To calculate whole-reservoir CH₄ emissions on each sampling date, upscaled whole-reservoir fluxes of CH₄ diffusion and ebullition were corrected for pool elevation based on surface area from four different data sources, and then were combined with CH₄ degassing. CH₄ fluxes were multiplied by 34 to capture their high 100-year global warming potential relative to CO₂ (Harrison et al., 2021) and the resulting values were expressed in CO₂-equivalents. Furthermore, to estimate whole-reservoir CH₄ flux over the entire surface area record for Douglas Reservoir (1980–2019), we scaled a median daily CH₄ flux for reservoirs >1 km², 46.4 mg CH₄ m⁻² d⁻¹ (Rosentreter et al., 2021), to monthly values of CO₂-equivalents and multiplied this by the corresponding surface area.

To construct a complete time series of surface area from 1980 to 2019 for Douglas Reservoir, we fitted a linear relationship ($R^2 = 0.98$) between GSW area and coincident reservoir elevation data reported in the Reservoir Operations data set (ResOpsUS) (Steyaert et al., 2022). This constructed record of historical surface area avoids data gaps caused by cloud cover and intervals between periods of satellite image acquisition. Then, to illustrate how much the variable surface area would impact calculations of CH₄ flux, we applied the median daily flux value for reservoirs from (Rosentreter et al., 2021). This is aggregated to a monthly value and multiplied by the average surface area in each month.

3. Results

3.1. Comparison of Surface Area and Littoral Area Based on Different Data Sources and Methods

A total of 1,891 US reservoirs having a cumulative surface area of 37,758 km² were identified for comparisons of total surface and littoral area from the HydroLAKES data set (i.e., those classified as reservoirs rather than natural lakes). The NID describes 35 times as many reservoirs (assuming all impounded water with non-zero storage and surface area values are reservoirs) with a cumulative surface area 4.7 times larger than HydroLAKES reservoirs. Distributions of surface areas and littoral areas showed some similarities across data sources and calculation methods used, despite describing different populations of waterbodies. Specifically, the distributions were all positively skewed, though median values differ by an order of 10 between the NID and both HydroLAKES and GSW (Figure 2a). HydroLAKES and GSW are biased toward larger reservoirs because these are limited to waterbodies with a reported extent of >0.1 km². In contrast, 70% of the reservoirs detailed in the NID have surface

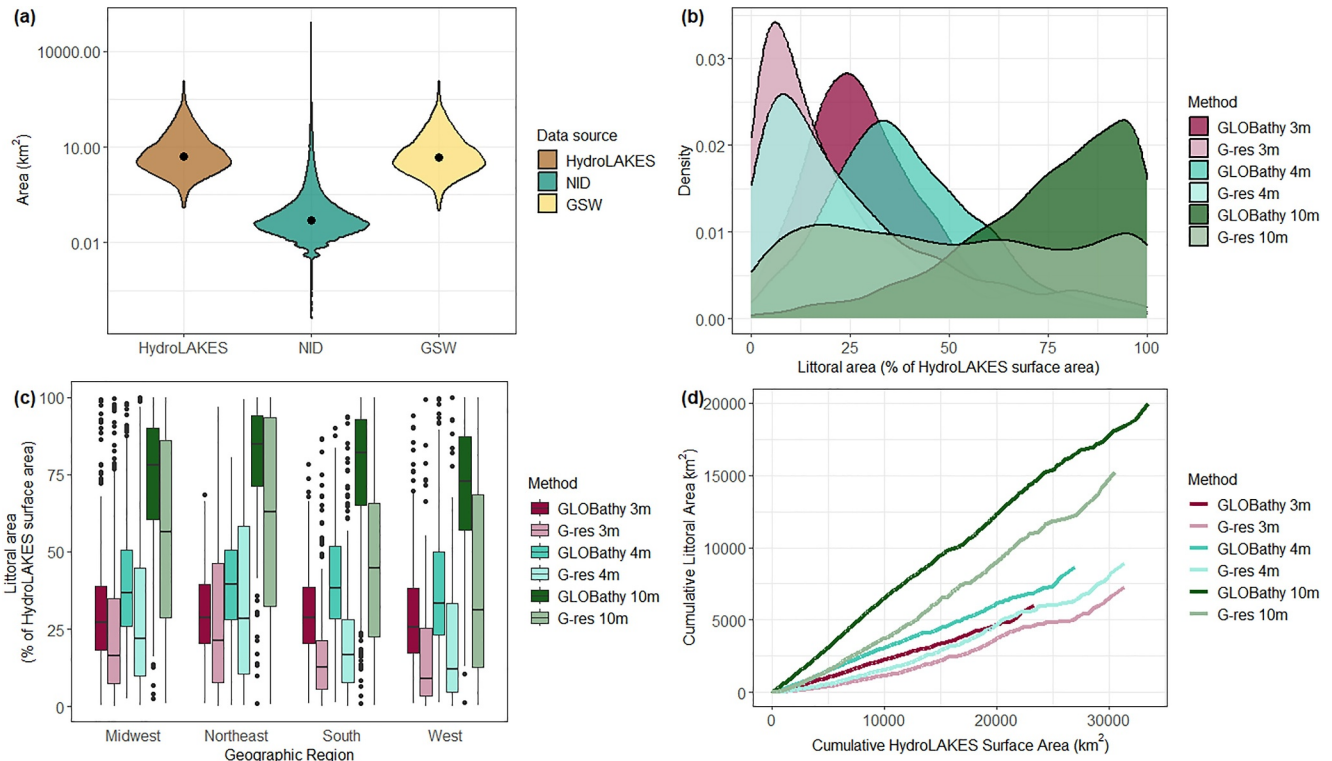


Figure 2. (a) Differences in positively skewed distributions of surface area according to different data sources (note logarithmic scale on y-axis) and the median surface area indicated with a marker and (b) how each method and depth threshold for estimating littoral area leads to different distributions of relative littoral area. Effects of the method and depth threshold on estimates of (c) relative littoral area across regions in the US, and (d) cumulative surface and littoral area for the US. Note that area is cumulatively summed in ascending order of reservoir max extent. This results in a slight uptick in cumulative littoral area at the right end of each line due to larger reservoirs.

areas $<0.1 \text{ km}^2$. Differences in medians evaluated using the Wilcoxon signed-rank test between SA_H , and SA_{GSW} were not statistically significant ($p > 0.05$), but differences between SA_H and SA_{NID} were statistically significant ($p < 0.0001$).

Estimating littoral area as the ratio of max and mean depth resulted in a broader distribution of relative littoral areas (i.e., larger standard deviation). Using this method, a higher portion of reservoirs had smaller relative littoral areas than those estimated from GLOBathy contours (Figure 2b). For all depth thresholds (3-m, 4-m, and 10-m), the G-res approach overestimated the mean littoral area compared to calculations using the GLOBathy data; at the 3-m threshold, the overestimation was 67%. The medians for relative littoral area were significantly different ($p < 0.0001$) based on Wilcoxon signed-rank tests between LA_{G-res} and LA_{Bath} (G-res and GLOBathy) for each depth threshold (Table 2).

Clear differences in median and interquartile ranges (IQR) of littoral area (Figure 2c) illustrate uncertainties in littoral area because of different estimation methods (i.e., GLOBathy contours vs. the equation from G-res documentation) and assumptions about depth thresholds. In all regions, the GLOBathy approach generally produced higher relative littoral areas compared to the G-res equation. The most extreme differences in median values and smallest overlaps in IQR between GLOBathy and G-res at any depth threshold were observed in the southern US, indicating the greatest sensitivity to the choice of both method and threshold. However, distributions were more similar in the Midwest and Northeast regions and for some individual reservoirs, higher values of relative littoral area were produced via G-res estimates. This suggests that the choice of method used to estimate littoral area may be more important in some regions compared to others. Comparing estimates from different methods across regions and purposes using the Kruskal-Wallis test, distributions of relative littoral area were significantly different across regions and purposes (both $p < 0.05$) for all methods and thresholds except when GLOBathy data and a 3-m threshold were used.

At the national scale, the method used to calculate littoral area (GLOBathy vs. G-res equation) and threshold (3-m, 4-m, or 10-m) has a large impact on aggregated littoral area in the US (Figure 2d). GLOBathy bathymetric data and a conservative 3-m depth threshold resulted in an estimate for total littoral area in US reservoirs of approximately 6,000 km², whereas a threshold of 10-m resulted in an estimate that is more than three times greater (nearly 20,000 km²).

3.2. Hindcasting Reservoir Dynamics

Fluctuation in total surface area for all US reservoirs included in water occurrence analysis ($n = 1,399$) were measured by the difference between the sum of maximum extent and the sum of area detected as water at each water occurrence threshold (Figure 3). At the 50% water occurrence threshold (i.e., for at least 50% of the satellite record), the total surface area for these reservoirs was 1,672 km² or 5% less than their max extent of 33,341 km². At the 90% water occurrence threshold, the total surface area was reduced by 6,908 km² (21%). There were clear patterns in how much reservoir area decreases based on size and use for hydroelectricity generation (Figures 3a and 3c). Less than 11% of reservoirs had a maximum extent >50 km², but these waterbodies accounted for roughly half of the decrease in total surface area at each water occurrence threshold. Similarly, reservoirs used for hydroelectricity (either as the primary purpose or multipurpose) accounted for fewer than one third of the reservoirs but more than half of the decrease in total surface area. Decreases in total surface area were more proportional for primary purpose, indicating that the large portion of surface area lost at higher water occurrence thresholds for multipurpose hydroelectric reservoirs is likely tied to the other purposes (besides generation) that primarily determine operations.

Patterns of relative surface area (change in area as a percentage of the maximum extent) varied substantially for different sizes and types of reservoirs (Figure 4). At low water occurrence thresholds (<50%), most reservoirs had a relative surface area between 90% and 100%. However, size was a distinguishing factor at higher thresholds (Figure 4a). At the 90% occurrence threshold the median relative surface area declined by 16.1% for large reservoirs (>200 km² according to their max extent) and 59.2% for small reservoirs (<1 km²). The increase in the IQR was also greatest for smaller reservoirs. This suggests that larger reservoirs tend to stay closer to their maximum extents than smaller reservoirs. This is consistent with our finding that smaller reservoirs exhibit greater relative variability in surface area.

Reservoirs with different purposes did not deviate in median and range of relative surface area until reaching higher (>60%) water occurrence thresholds (Figures 4b and 4c). Even at a 60% water occurrence threshold, meaning water must be detected more than half of the satellite record, the relative surface area is generally above 75%. Additionally, median values of relative surface area for all purposes were within 5% of each other and the IQRs are small, spanning <18% at this threshold. At the 90% water occurrence threshold, differences are more substantial; median relative surface area of non-hydroelectric reservoirs (73%) is lower and IQR is greater (spanning 48%) than those that may be multi-purpose but are used for hydroelectricity (median = 80%, IQR span = 30%). In particular, reservoirs that primarily support irrigation and fisheries are much lower (median = 56–59%, IQR span = 42–46%). This indicates that variation in the relative surface area of hydroelectric reservoirs is lower than those that do not support hydroelectric generation.

On a regional basis, median relative surface area was between 60% and 91% (Figure 5) and the spreads of relative surface area were wide; only five regions had IQR spanning less than 25%. Notably, medians were lowest in the Mid-Atlantic, Rio Grande, and Great Basin regions (HUC 02, 13, and 16, respectively), ranging from 35% to 52% (mean = 39%–49%). This means that for the average reservoir in these regions, less than half of the area within the maximum extent was inundated at least 90% of the time. Both the Mid-Atlantic and Great Basin regions had an IQR >50%, reflecting their particularly high diversity of reservoir types and areal fluctuations. In contrast, the median of the Souris-Red-Rainy region (HUC 09) was 91% and the IQR was only 12%.

We investigated correlations between climate, hydrological, topographical characteristics and relative surface area that may be driven by regional differences in hydrology or climate. Graphical comparisons show some distinction among reservoirs with respect to runoff (Figure S2 in Supporting Information S1), however, all variables were weakly correlated. There were no statistically significant correlations at the 95% confidence level, indicating that there was no strong evidence of a simple, monotonic relationship between relative water-surface occurrences and runoff, temperature or elevation. However, there was a clear difference in variability of relative surface depending on the amount of runoff. Surface area was consistently near 100% for reservoirs with runoff

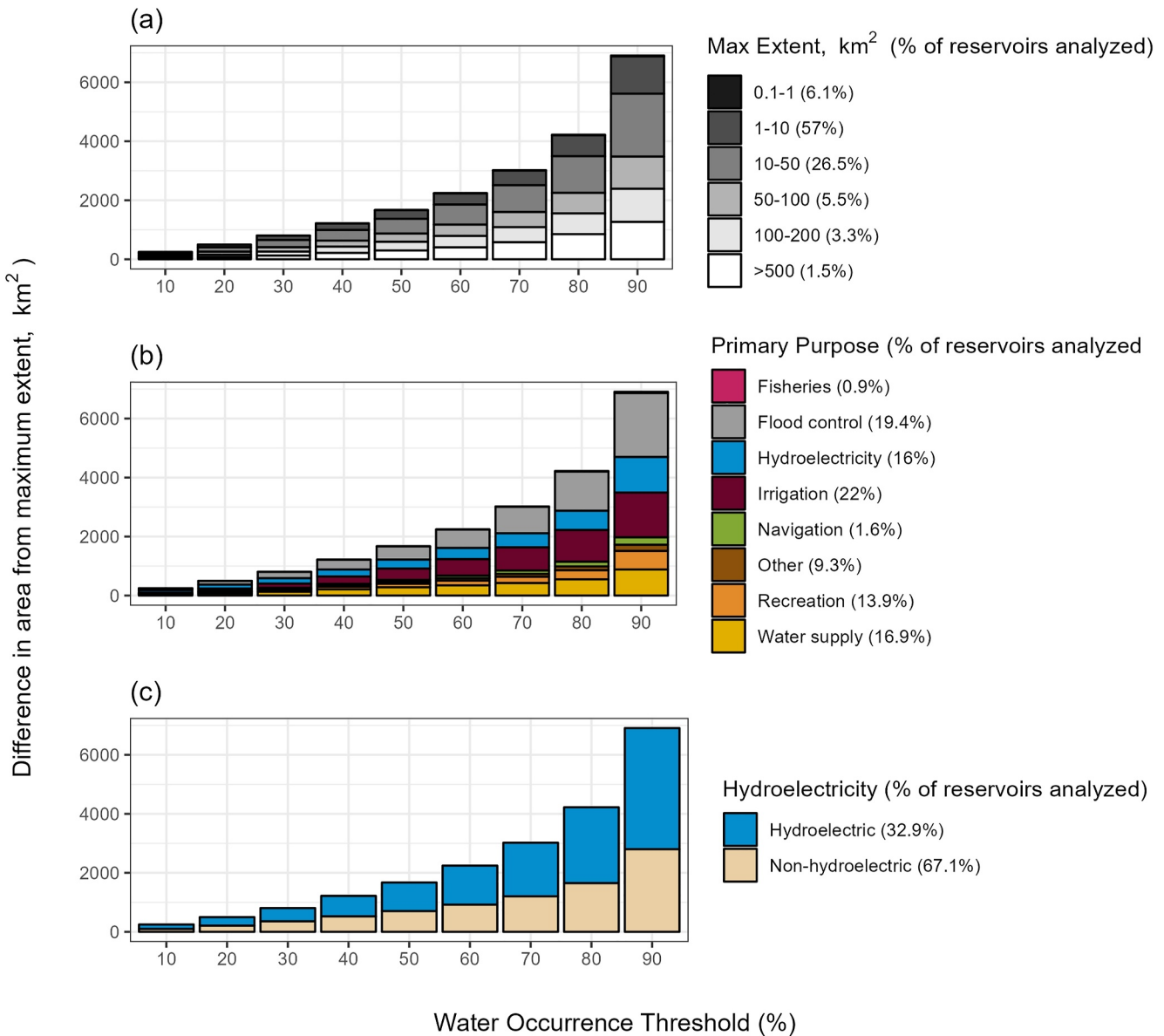


Figure 3. Decreases in surface area (relative to the maximum extent) with respect to different thresholds of water occurrence, compared across (a) surface areas (from HydroLAKES), (b) primary purposes and (c) hydroelectric versus non-hydroelectric reservoirs. A threshold of 50% is considered low water occurrence, as this represents pixels where water is not detected for at least half of the satellite record.

>1,000 mm yr⁻¹, especially at the 50% and 70% water-occurrence thresholds, whereas the relative surface area for reservoirs with lower annual runoff was highly variable.

The temporal behavior of reservoir surface area between 1984 and 2021 was analyzed to provide two additional perspectives on the changes in reservoir surface area over time using measures of monthly and yearly recurrence data from the GSW data set (Figure 6). Seasonal fluctuations in surface area were reflected in the number of months per year when water was detected, averaged over the extent of the HydroLAKES boundary (Figure 6a). Low values indicate that large portions of the reservoir are only detected as water for a few months. Only 51 (3.6%) of the US reservoirs analyzed had a monthly recurrence of less than 6 months and most of these ($n = 43$) have a surface area <10 km². In contrast, the largest reservoirs consistently had high rates of monthly recurrence.

Additionally, the year-to-year variability of water presence (Figure 6b) in smaller reservoirs varied much more (from 40% to 100%) whereas larger reservoirs remained near full pool, at >90% recurrence. Patterns were similar

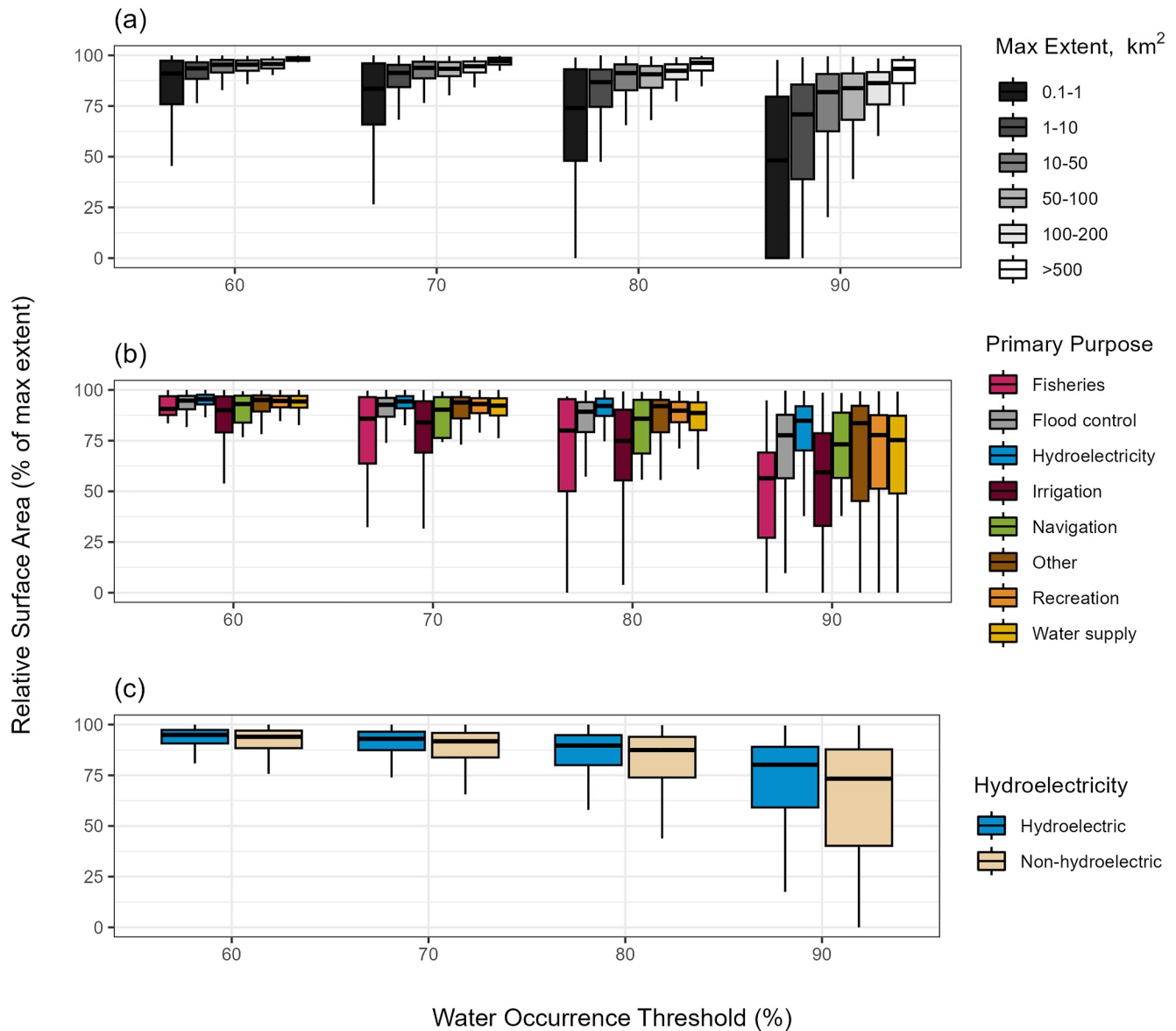


Figure 4. Relative surface area (as a percentage of the maximum extent) with respect to different thresholds of water occurrence, compared across (a) surface areas (from HydroLAKES), (b) primary purposes and (c) hydroelectric versus non-hydroelectric reservoirs. Only water occurrence thresholds >50% are shown because distributions for all reservoir categories are very similar at lower thresholds, with IQR of relative surface area falling generally between 90% and 100%.

for hydroelectric and non-hydroelectric reservoirs, though the range for non-hydroelectric reservoirs extended much lower for both monthly and yearly recurrence.

3.3. Connections Between Variable Reservoir Surface Area and Measured and Estimated Methane Emissions From Douglas Reservoir

Water level at Douglas Reservoir varies by up to ~15 m over the course of a year between fall drawdown (~mid-November) and spring refill (~early April), according to TVA operating guidelines. During periods of drawdown, the percentage of the reservoir that is in the littoral zone (assuming a depth ≤ 3 m) increases due to the bathymetry of the reservoir (Figure 7, Figure S1 in Supporting Information S1). For instance, when the reservoir is at winter pool, the reservoir surface area in the littoral zone is 21% (GRanD/HydroLAKES) to 26% (NHD + HR), compared to <18% in the summer when the reservoir is at full-pool elevation. Depending on the bathymetry and source of reservoir geometry, the total area of the littoral zone either increases with small drawdown depths and

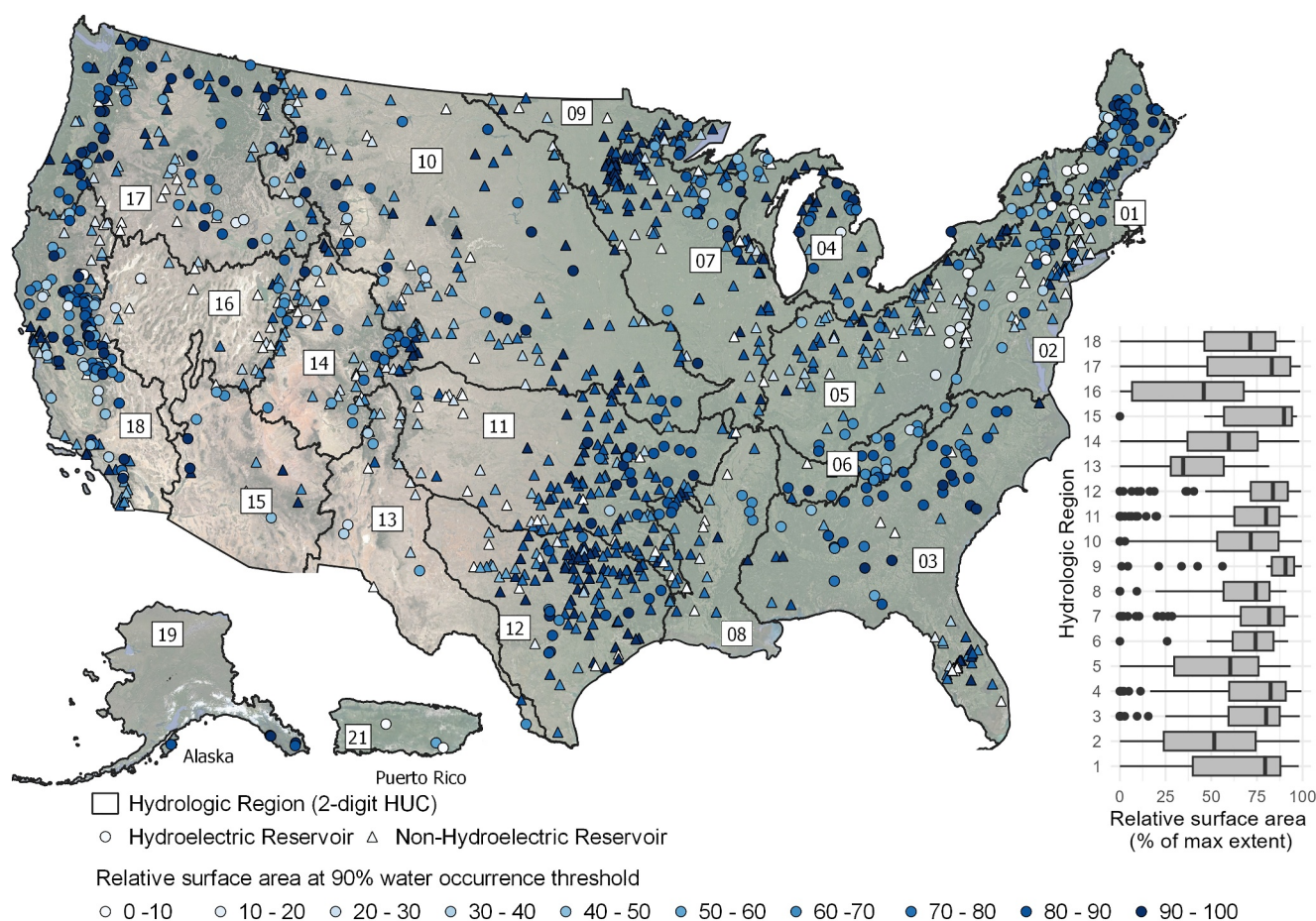


Figure 5. Distribution of reservoirs and variability in relative surface area at the 90% water-occurrence threshold. The map shows locations of 1,399 reservoirs in the HydroLAKES data set which are shaded by a blue color ramp according to the relative reservoir surface area changes at a 90% water-occurrence threshold. Boxplots describe the distribution of relative surface area of the reservoirs within each two-digit hydrologic region at the 90% water occurrence threshold. Note that HydroLAKES does not include any reservoirs for hydrologic region 20 (Hawaii) and regions 19 and 21 are excluded from the boxplot due to the low number of reservoirs in each region.

decreases when drawdown > 12 m (using the GRanD/HydroLAKES boundary) or linearly decreases at all depths (using the NHD or NHD + HR boundary). Hence, the relative importance of CH₄ emissions from the littoral zone, where CH₄ bubbling tends to dominate, likely increases during periods of drawdown due to higher proportions of the water at shallower depths.

Upscaled CH₄ emissions that depend on total surface area and relative littoral area can result in substantial variability. Comparing four different data sources of surface area for Douglas Reservoir, whole-reservoir CH₄ emissions varied by nearly two-fold (up to 85%) solely based on the source of surface area data used (Figure 8a). Significant temporal variations in upscaled CH₄ emissions from Douglas Reservoir were also detected (Figure 8b). Estimated CH₄ emissions ranged from 5.8×10^3 kg CO₂-eq day⁻¹ at full pool in summer 2022 (GRanD/HydroLakes surface area data) to as high as 1.3×10^5 kg CO₂-eq day⁻¹ during winter pool in December 2021 (NHD + HR surface area data). However, even within a specific sampling date, the upscaled GHG emission estimate varied widely depending on the data source used to calculate pool-corrected surface area. Relative to the GRanD/HydroLAKES surface area, GHG estimates differ by -0.5%, 5.1%, and 5.3% (December 2021), 75%, 82%, and 85% (May 2022), and 30%, 37%, and 38% (October 2022) for the NID, NHD, and NHD + HR data sets, respectively.

The effect of surface area variability on upscaled CH₄ emission estimates is further illustrated for Douglas Reservoir using a time series of monthly and annual average surface area (Figure 9). Using the record of daily reservoir elevation between 1980 and 2019 from ResOpsUS and the relationship between area and elevation, the

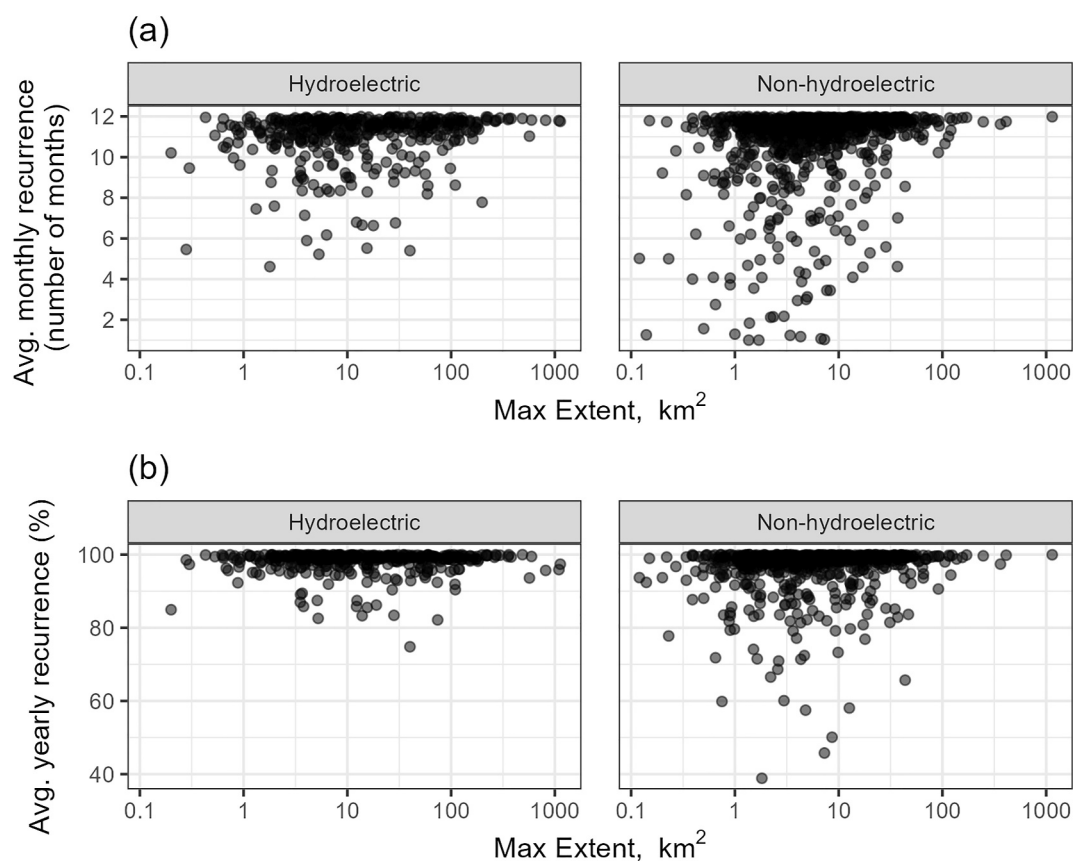


Figure 6. Comparison of the temporal patterns in surface water presence by reservoir size; (a) Average number of months with water present, averaged over the pixels within the HydroLAKES boundary and across the record from 1984 to 2021. (b) Average yearly recurrence which describes the percentage of time that water is detected from 1 year to the next. Higher recurrence values indicate that water is consistently detected during the same months over the 1984–2021 record. Note the log-transformed x-axis.

monthly average surface area of Douglas Reservoir fluctuated between 48 km² a maximum of 107 km². Estimated whole-reservoir monthly CH₄ fluxes ranged from 2.32 × 10⁶ kg CO_{2-eq} month⁻¹ to 5.07 × 10⁶ kg CO_{2-eq} month⁻¹; with a median flux value of 3.72 × 10⁶ kg CO_{2-eq} month⁻¹ across the 40-year period (Figure 9a). Seasonal fluctuation in surface area is clear, with median monthly surface area and corresponding whole-reservoir CH₄ flux ranging from 58 km² to 2.78 × 10⁶ kg CO_{2-eq} (January) to 102 km² and 4.83 × 10⁶ kg CO_{2-eq} (June) (Figure 9b). The histogram of whole-reservoir CH₄ flux shows the wide spread in monthly scaled fluxes (Figure 9c). While these calculations illustrate the impact of changing surface area over time, they do not reflect variations in emission rates due to phenological shifts or long-term changes in reservoir biogeochemistry. However, these factors could potentially interact with surface area fluctuations (e.g., changes in hydrostatic pressure), as seen in the field sampling data from Douglas Reservoir, which could significantly alter the estimated emissions.

4. Discussion

4.1. Differences Among Data Sets

The data sources and methods examined in this study produced highly variable descriptions of reservoir and littoral area in the US. While SA_{GSW} and SA_H were within 3% of each other, these estimates of total area were only 20% of what is described in the NID. Similarly, the most conservative depth threshold of 10 m for littoral area resulted in average and cumulative values that were roughly four times greater than those estimated using a 3-m threshold. These substantial differences in sources and methods can significantly impact individual reservoir upscaling to regional or global estimates of GHG emissions. The Douglas Reservoir case study demonstrated how

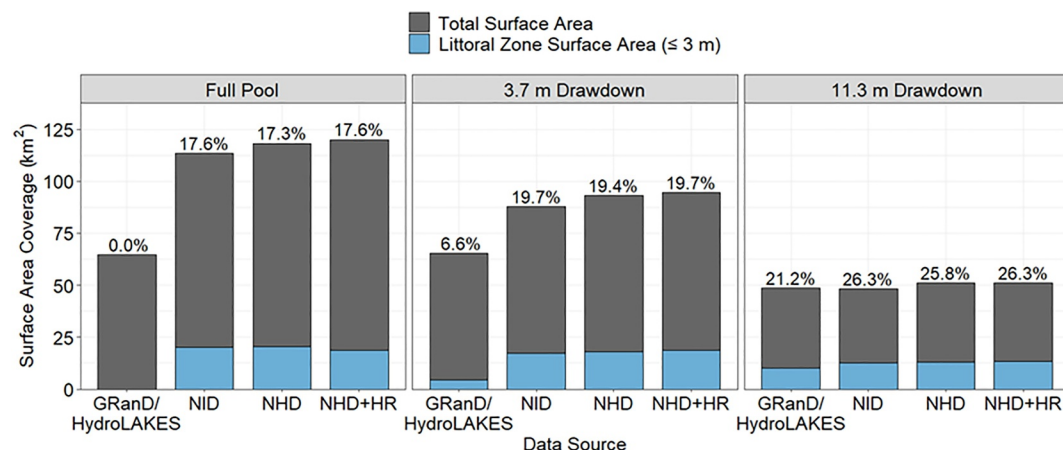


Figure 7. The total surface area of Douglas Reservoir in east Tennessee, USA, derived from four different data sources (GRanD/HydroLAKES, NID, NHD, NHD + HR) as indicated by gray bars, and the proportion of surface area within the littoral zone (≤ 3 m), as indicated by blue bars (the percentage of total surface area as littoral area is also shown as a value above each bar). Panels show how total surface area and corresponding littoral area change as a function of drawdown that correspond to the three dates on which GHG emissions were measured in Douglas Reservoir (left = full pool (April 2022); center = 3.7 m drawdown (October 2022); right = 11.3 m drawdown (December 2021)). Calculation of total surface area and proportion littoral area for all three time points are based on empirical bathymetric data and hypsographic curves of Douglas Reservoir.

differences in estimates of surface area from different data sources can affect upscaled CH_4 emission estimates by up to nearly two-fold, illustrating the importance of acknowledging the underlying assumptions when tying large-scale summaries to a particular inventory of waterbodies.

Summaries of reservoir area and variability (including this study) must acknowledge the limitations of using remotely sensed data to describe surface area. Records based on satellite imagery may be impacted by acquisition schedules, cloud cover, or characteristics like poor water clarity or dense emergent vegetation that make it

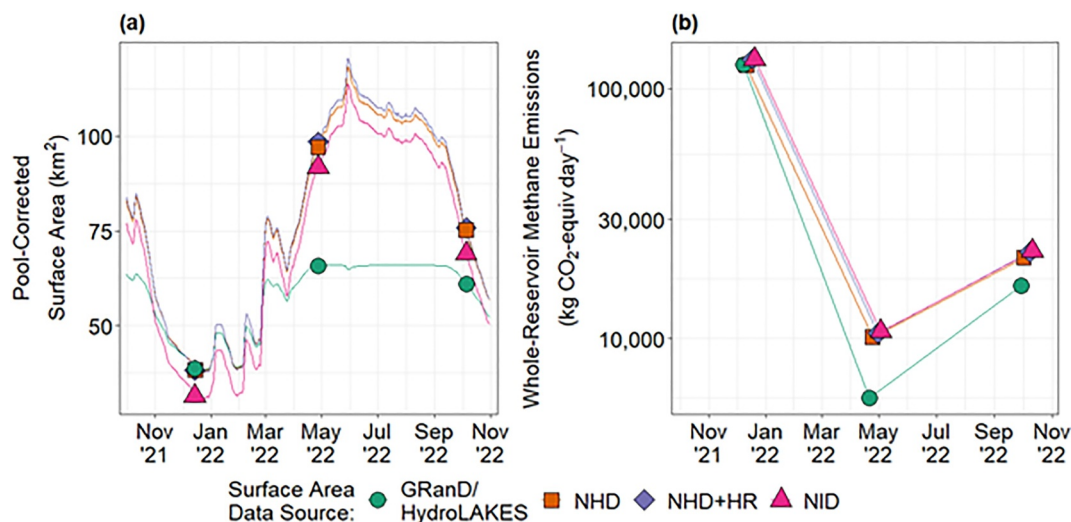


Figure 8. Variation in Douglas Reservoir on three sampling visits from December 2021 through October 2022. (a) Pool-corrected surface area, based on different data sources, empirical hypsographic curves, and pool elevations. Lines represent surface area on a daily basis while points highlight the area on specific sampling dates. (b) Whole-reservoir CH_4 emissions (as CO_2 equivalents). Use the pool-corrected surface area from each respective data source. Individual points in (b) are slightly horizontally jittered for visual clarity, but all calculations stem from the same series of empirical, in-situ GHG emissions measurements. Note (b) uses a log-transformed y-axis.

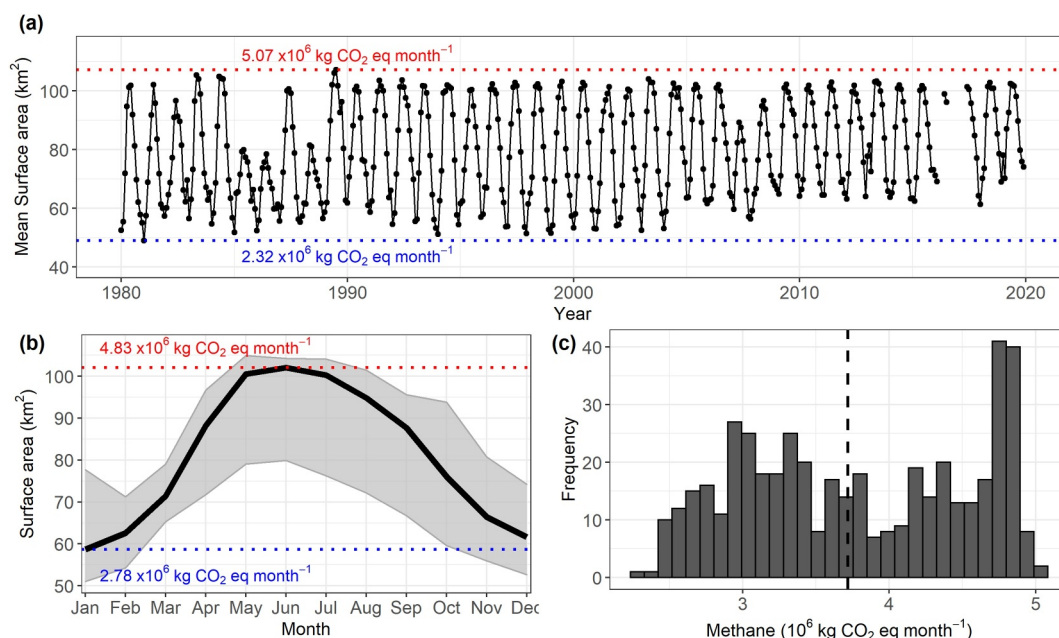


Figure 9. (a) Average monthly surface area of Douglas Reservoir from 1980 to 2019 with whole-reservoir scaled CH_4 fluxes (in $\text{kg CO}_2\text{-eq}$) for the minimum and maximum months during this period shown in blue and red, respectively and (b) median (black line) and 95% confidence intervals (gray) of surface area on a monthly basis, with whole-reservoir scaled CH_4 fluxes (in $\text{kg CO}_2\text{-eq}$) shown in blue for January (the month with the lowest median surface area) and red for June (the month with the greatest median surface area). Additionally, (c) the frequency distribution of monthly CH_4 fluxes from 1980 to 2019 is shown, with the median monthly value shown with the black dashed line.

challenging to accurately apply common water-detection algorithms. However, satellite and airborne remote sensing may offer a path toward better partitioning of the littoral zone by identifying vegetated areas and creating high-resolution bathymetry maps (e.g., Lidar). The littoral area is currently used as a predictor for CH_4 ebullition in the G-res model (Prairie et al., 2017), and thus better characterization of the littoral area via satellite imagery will improve our ability to upscale CH_4 ebullition rates (Juutinen et al., 2003).

Some patterns in the variability of reservoir surface area based on reservoir size, purpose, or region may be influenced by which data set is used and how it defines a reservoir. Aside from the comparison to surface area in the NID, our national-scale analysis is limited to US reservoirs which may bias the distributions and relative surface area tied to the HydroLAKES data set, as this data set only includes waterbodies with surface areas greater than 0.1 km^2 . The lack of clear distinctions between reservoirs, lakes, and rivers can create confusion when comparing HydroLAKES and other US or global reservoir data sets. For example, one data set may not recognize an impounded waterbody as a reservoir and instead consider it a river, even though there is storage reported by dam inventories. Additionally, models trained on measurements and characteristics of lentic reservoir systems may not be applicable to lotic, riverine reservoirs. Greater consistency in how waterbodies are described and categorized can reduce uncertainty in large-scale estimates and ensure that appropriate methods are used to estimate GHG emissions.

4.2. Patterns of Areal Variability

Our analysis revealed that larger reservoirs and reservoirs with hydroelectricity as a primary or secondary purpose make up the majority of fluctuating total surface area as evident by the largest share of decreases in area over all water occurrence thresholds. However, these same groups of reservoirs exhibit less variability in relative surface area (i.e., fluctuate less relative to their own maximum extent) compared to smaller reservoirs and those serving non-hydroelectric purposes. These findings are consistent with the results of other recent studies that have observed a greater relative drawdown in smaller reservoirs (Bonnema et al., 2022; Keller et al., 2021). While total surface area fluctuation is crucial for understanding ecological and physical processes relevant to habitat, recreation, and safety, relative surface area fluctuation is key to estimating dynamics in GHG emissions and different

pathways that are likely dependent on an individual waterbody's surface area characteristics. Reservoir size and purpose interact in explaining patterns of relative area variability. For instance, reservoirs used for irrigation and fisheries tend to be smaller in size because they support seasonal, rather than inter-annual, water demands while hydroelectric reservoirs tend to be larger in size and have smaller relative drawdown areas since they support both inter-annual and sub-annual (to sub-daily) electricity generation needs.

Despite general patterns in surface area based on reservoir type, there still can be large variability in relative surface area within these groups. The large IQRs shown in Figure 4 highlight the importance of considering both size and purpose. As such, variability in surface area and the littoral area within a reservoir may not be easily generalizable based on the simple distinctions of size, purpose, or geography. Changes in reservoir water levels (and consequently the surface extent and littoral area) may be caused by changes in hydrologic inputs or in reservoir operational regimes (Harrison et al., 2021), and these fluctuations occur on scales ranging from sub-daily and daily fluctuations (i.e., hydropeaking), to seasonal drawdown, to inter-annual wet/dry months (Jager et al., 2023). These water-level changes have been associated with potential changes in GHG emissions. For instance, drawdowns lead to decreased hydrostatic pressure and increased CH₄ emissions (Beaulieu et al., 2018; Jager et al., 2022; Kosten et al., 2018). Our study did not attempt to evaluate the causes or drivers of variability in surface extent; however, the identification of factors that contribute most to variability are important to anticipate how GHG emissions may change in the future based on planned management actions or identifying best practices for mitigating emissions (Jager et al., 2022, 2023).

Measures of seasonality in surface area also reveal that, when relative measures are used, smaller reservoirs and non-hydroelectric reservoirs exhibit larger ranges in both the number of months when water is detected and in year-to-year water recurrence. Additionally, it is not enough to consider the range of surface area (i.e., minimum and maximum extents) or simply measure emissions multiple times; we also need to account for how much time waterbodies spend at different water levels and surface area conditions. This was illustrated for Douglas Reservoir, which spends just 3 months of the year within 10% of the full reservoir extent (Figure 9). Although collections of GHG measurements used to train empirical models span many types and sizes of reservoirs, they do not yet account for drawdown status or seasonal or annual fluctuations. Seasonal drawdown patterns could be factored into the temporal aggregation or annualization process that is often used to develop empirical relationships, especially since the lack of synoptic GHG measurements results in collections with different measurement durations and frequencies.

Investigation of seasonal (and finer) time scales of drawdown and their influences on reservoir GHG emissions is also critical to better understand driving forces for ebullition. Interactions with seasonally varying hydrodynamics (i.e., drawdown-influenced changes in hydrostatic pressure and thermal stratification) and biogeochemical processes could have compounding effects on ebullition or other pathways for GHG emissions. Although this study did not analyze diurnal variations in water level, future research incorporating high-frequency field or remote-sensing measurements in reservoirs could build on recent studies that show significant diurnal fluctuations in downstream GHG emissions (Calamita et al., 2021). Such research can enhance our understanding of short-term disturbances, like episodic water-column mixing, storm events, or intense algal blooms on surface water GHG emissions.

Regional patterns of relative surface area largely reflect differences in the types of reservoirs (size and the primary operational purpose) that tend to dominate certain regions rather than hydro-climatological conditions. Regions with the lowest median and largest range in relative surface area are located across the middle and lower latitudes of the US and have very different hydro-climates, but they are largely made up of smaller irrigation and water supply reservoirs and just a few very large reservoirs (Figure S3 in Supporting Information S1). In contrast, in many of the regions with a higher share of large flood control or hydroelectric reservoirs (i.e., HUCs 01, 03, 04, 11, 12), relative surface area tends to stay near the maximum. Differences in regional surface area dynamics, coupled with observed regional patterns in the surface morphologies of reservoirs could further complicate comparisons of GHG emissions across waterbodies (Hansen et al., 2023). Despite latitudinal patterns observed in GHG measurements, the link between reservoir location, surface area variability, and GHG emissions may not be so straight-forward.

5. Conclusions

Empirically based models of GHG emissions from reservoirs often use a static description of total surface area and/or littoral area for upscaling calculations. However, we have shown there are statistically significant differences in these foundational metrics depending on the data set and that surface area changes for many reservoirs over seasonal or longer time frames. Limitations and uncertainties associated with typical GHG modeling and upscaling methods that are based on static descriptions of total surface area and littoral area can stem from differences or lack of specificity in data sets or assumptions used to define littoral zones. Current practices of summarizing reservoir-wide emissions do not reflect the variation in emissions that is tied to fluctuations in water levels and areas.

Advances in understanding the dynamic nature of underlying biogeochemical processes and resulting CH₄ emissions in the littoral zone will likely come through high-frequency measurements and mechanistic or process-based modeling that can represent temporally dynamic changes in surface area, depth, and littoral area. These models are challenging for individual waterbodies because of input data requirements; however, emerging data sets that provide high resolution and global coverage of bathymetry or water surface (e.g., Surface Water and Ocean Topography satellite data, bathymetric lidar, etc.) may help overcome barriers to efficient large-scale assessment of littoral-area dynamics. Additionally, other reservoir drivers and processes including hydroclimate conditions, carbon burial, eutrophication (Kumar et al., 2023), and emergent vegetation (Kyzivat et al., 2022) are critical to GHG emissions and should be accounted for alongside variability in area. More detailed descriptions of these factors over space and time will improve our understanding of GHG emissions and ability to compare different systems and ultimately predict GHG emissions in the future as waterbody areas fluctuate or experience permanent shifts in surface or littoral areas.

Data Availability Statement

The metrics obtained from the GSW data set and comparisons between different reservoir data sets are available through Zenodo (Hansen & Iftikhar, 2024); <https://doi.org/10.5281/zenodo.11205708>. Data obtained for Douglas Reservoir through field sampling are available through Zenodo (Pilla et al., 2023); <https://doi.org/10.5281/zenodo.7915527>.

References

- Abatzoglou, J. T., Dobrowski, S. Z., Parks, S. A., & Hegewisch, K. C. (2018). TerraClimate, a high-resolution global dataset of monthly climate and climatic water balance from 1958–2015. *Scientific Data*, 5(1), 1–12. <https://doi.org/10.1038/sdata.2017.191>
- Bastviken, D., Cole, J., Pace, M., & Tranvik, L. (2004). Methane emissions from lakes: Dependence of lake characteristics, two regional assessments, and a global estimate. *Global Biogeochemical Cycles*, 18(4). <https://doi.org/10.1029/2004gb002238>
- Beaulieu, J. J., Balz, D. A., Birchfield, M. K., Harrison, J. A., Nietch, C. T., Platz, M. C., et al. (2018). Effects of an experimental water-level drawdown on methane emissions from a eutrophic reservoir. *Ecosystems*, 21(4), 657–674. <https://doi.org/10.1007/s10021-017-0176-2>
- Beaulieu, J. J., McManus, M. G., & Nietch, C. T. (2016). Estimates of reservoir methane emissions based on a spatially balanced probabilistic survey. *Limnology & Oceanography*, 61(S1), S27–S40. <https://doi.org/10.1002/lno.10284>
- Bevelhimer, M., Stewart, A., Fortner, A., Phillips, J., & Mosher, J. (2016). CO₂ is dominant greenhouse gas emitted from six hydropower reservoirs in southeastern United States during peak summer emissions. *Water*, 8(1), 15. <https://doi.org/10.3390/w8010015>
- Bonnema, M., David, C. H., Frasson, R. P. d. M., Oaida, C., & Yun, S. H. (2022). The global surface area variations of lakes and reservoirs as seen from satellite remote sensing. *Geophysical Research Letters*, 49(15). <https://doi.org/10.1029/2022gl098987>
- Calamita, E., Siviglia, A., Gettel, G. M., Franca, M. J., Winton, R. S., Teodoru, C. R., et al. (2021). Unaccounted CO₂ leaks downstream of a large tropical hydroelectric reservoir. *Proceedings of the National Academy of Sciences*, 118(25), e2026004118. <https://doi.org/10.1073/pnas.2026004118>
- Cantonati, M., & Lowe, R. L. (2014). Lake benthic algae: Toward an understanding of their ecology. *Freshwater Science*, 33(2), 475–486. <https://doi.org/10.1086/676140>
- Danielson, J. J., & Gesch, D. B. (2011). Global multi-resolution Terrain elevation data 2010 (GMTED2010) [Dataset]. <https://doi.org/10.5066/F7J38R2N>
- Deemer, B. R., Harrison, J. A., Li, S. Y., Beaulieu, J. J., Delsonro, T., Barros, N., et al. (2016). Greenhouse gas emissions from reservoir water surfaces: A new global synthesis. *BioScience*, 66(11), 949–964. <https://doi.org/10.1093/biosci/biw117>
- Downing, J. A., Prairie, Y. T., Cole, J. J., Duarte, C. M., Tranvik, L. J., Striegl, R. G., et al. (2006). The global abundance and size distribution of lakes, ponds, and impoundments. *Limnology & Oceanography*, 51(5), 2388–2397. <https://doi.org/10.4319/lo.2006.51.5.2388>
- Geraldes, A. M., & Boavida, M.-J. (2005). Seasonal water level fluctuations: Implications for reservoir limnology and management. *Lakes and Reservoirs: Research and Management*, 10(1), 59–69. <https://doi.org/10.1111/j.1440-1770.2005.00257.x>
- Hansen, C., & Iftikhar, B. (2024). US reservoir surface and littoral area [Dataset]. *Zenodo*. <https://doi.org/10.5281/zenodo.11205708>
- Hansen, C., & Matson, P. (2022). Hydropower infrastructure - LAkes, reservoirs, and rivers (HILARRI). [Dataset]. <https://doi.org/10.21951/HILARRI/1960141>
- Hansen, C., Matson, P., & Griffiths, N. (2023). Diversity in reservoir surface morphology and climate limits ability to compare and upscale estimates of greenhouse gas emissions. *The Science of the Total Environment*, 893, 164851. <https://doi.org/10.1016/j.scitotenv.2023.164851>

Acknowledgments

This research was supported by the U.S. Department of Energy (DOE), Office of Energy Efficiency and Renewable Energy, Water Power Technologies Office, program manager Dr. Charles Scaife. We would like to express our gratitude to the sampling crew for collecting the data for Douglas Reservoir used in this paper (C. S. Faehndrich, A. M. Fortner, R. T. Jett, M. W. Jones, N. J. Jones, and J. R. Phillips).

- Harrison, J. A., Prairie, Y. T., Mercier-Blais, S., & Soued, C. (2021). Year-2020 global distribution and pathways of reservoir methane and carbon dioxide emissions according to the greenhouse gas from reservoirs (G-res) model. *Global Biogeochemical Cycles*, 35(6), 1–14. <https://doi.org/10.1029/2020gb006888>
- Henson, E. B. (1993). Estimating the areal extent of the littoral zone in lakes. *Internationale Vereinigung für theoretische und angewandte Limnologie: Verhandlungen*, 25(1), 414–418. <https://doi.org/10.1080/03680770.1992.11900153>
- Hijmans, R. J., Bivand, R., Forner, K., Ooms, J., Pebesma, E., & Sumner, M. D. (2022). terra: Spatial data analysis [Software]. *R Package version 1.8-5*. <https://doi.org/10.32614/CRAN.package.terra>
- Jager, H. I., Griffiths, N. A., Hansen, C. H., King, A. W., Matson, P. G., Singh, D., & Pilla, R. M. (2022). Getting lost tracking the carbon footprint of hydropower. *Renewable and Sustainable Energy Reviews*, 162, 112408. <https://doi.org/10.1016/j.rser.2022.112408>
- Jager, H. I., Pilla, R. M., Hansen, C. H., Matson, P. G., Iftikhar, B., & Griffiths, N. A. (2023). Understanding how reservoir operations influence methane emissions: A conceptual model. *Water*, 15(23), 4112. <https://doi.org/10.3390/w15234112>
- Juutinen, S., Alm, J., Larmola, T., Huttunen, J. T., Morero, M., Martikainen, P. J., & Silvola, J. (2003). Major implication of the littoral zone for methane release from boreal lakes. *Global Biogeochemical Cycles*, 17(4). <https://doi.org/10.1029/2003gb002105>
- Keller, P. S., Marcé, R., Obrador, B., & Koschorreck, M. (2021). Global carbon budget of reservoirs is overturned by the quantification of drawdown areas. *Nature Geoscience*, 14(6), 402–408. <https://doi.org/10.1038/s41561-021-00734-z>
- Khaza'ei, B., Read, L. K., Casali, M., Sampson, K. M., & Yates, D. N. (2022). GLOBathy, the global lakes bathymetry dataset. *Scientific Data*, 9(1), 36. <https://doi.org/10.1038/s41597-022-01132-9>
- Kosten, S., van den Berg, S., Mendonça, R., Paranaíba, J. R., Roland, F., Sobek, S., et al. (2018). Extreme drought boosts CO₂ and CH₄ emissions from reservoir drawdown areas. *Inland waters*, 8(3), 329–340. <https://doi.org/10.1080/20442041.2018.1483126>
- Kumar, A., Kumar, A., Chaturvedi, A. K., Joshi, N., Mondal, R., & Malyan, S. K. (2023). Greenhouse gas emissions from hydroelectric reservoirs: Mechanistic understanding of influencing factors and future prospect. *Environmental Science and Pollution Research*, 1–18. <https://doi.org/10.1007/s11356-023-25717-y>
- Kyzivat, E. D., Smith, L. C., Garcia-Tigreros, F., Huang, C., Wang, C., Langhorst, T., et al. (2022). The importance of lake emergent aquatic vegetation for estimating arctic-boreal methane emissions. *Journal of Geophysical Research: Biogeosciences*, 127(6), e2021JG006635. <https://doi.org/10.1029/2021jg006635>
- Lehner, B., Liermann, C. R., Revenga, C., Vörösmarty, C., Fekete, B., Crouzet, P., et al. (2011). High-resolution mapping of the world's reservoirs and dams for sustainable river-flow management. *Frontiers in Ecology and the Environment*, 9(9), 494–502. <https://doi.org/10.1890/100125>
- Messenger, M. L., Lehner, B., Grill, G., Nedeva, I., & Schmitt, O. (2016). Estimating the volume and age of water stored in global lakes using a geo-statistical approach. *Nature Communications*, 7(2), 13603. <https://doi.org/10.1038/ncomms13603>
- Pebesma, E. (2018). Simple features for R: Standardized support for spatial vector data. *The R Journal*, 10(1), 439–446. <https://doi.org/10.32614/rj-2018-009>
- Pekel, J.-F., Cottam, A., Gorelick, N., & Belward, A. S. (2016). High-resolution mapping of global surface water and its long-term changes. *Nature*, 540(7633), 418–422. <https://doi.org/10.1038/nature20584>
- Pilla, R. M., Faehndrich, C. S., Fortner, A. M., Jett, R. T., Jones, M. W., Jones, N. J., et al. (2023). Rates and drivers of carbon emissions from hydropower reservoirs in the southeastern United States [Dataset]. *Zenodo*. <https://doi.org/10.5281/zenodo.7915527>
- Prairie, Y., Alm, J., Harby, A., Mercier-Blais, S., & Nahas, R. (2017). The GHG reservoir tool (G-res tool) technical documentation v2.1. Retrieved from <https://www.hydropower.org/publications/the-ghg-reservoir-tool-g-res-technical-documentation>
- R Core Team. (2023). R: A language and environment for statistical computing [Software]. *R Foundation for Statistical Computing*. Retrieved from: <https://www.R-project.org/>
- Rosentreter, J. A., Borges, A. V., Deemer, B. R., Holgerson, M. A., Liu, S., Song, C., et al. (2021). Half of global methane emissions come from highly variable aquatic ecosystem sources. *Nature Geoscience*, 14(4), 225–230. <https://doi.org/10.1038/s41561-021-00715-2>
- Scherer, L., & Pfister, S. (2016). Hydropower's biogenic carbon footprint. *PLoS One*, 11(9), e0161947. <https://doi.org/10.1371/journal.pone.0161947>
- Seekell, D., Cael, B., Norman, S., & Byström, P. (2021). Patterns and variation of littoral habitat size among lakes. *Geophysical Research Letters*, 48(20). <https://doi.org/10.1029/2021gl095046>
- Shi, W., Chen, Q., Zhang, J., Lu, J., Chen, Y., Pang, B., et al. (2021). Spatial patterns of diffusive methane emissions across sediment deposited riparian zones in hydropower reservoirs. *Journal of Geophysical Research: Biogeosciences*, 126(3), e2020JG005945. <https://doi.org/10.1029/2020jg005945>
- Steyaert, J. C., Condon, L. E., Turner, S. W. D., & Voisin, N. (2022). ResOpsUS, a dataset of historical reservoir operations in the contiguous United States. *Scientific Data*, 9(1), 34. <https://doi.org/10.1038/s41597-022-01134-7>
- Tennessee Vally Authority (TVA). (2023). Douglas reservoir: *Reservoir Health Ratings*. Retrieved from <https://www.tva.com/environment/environmental-stewardship/water-quality/reservoir-health-ratings/douglas-reservoir>
- United States Army Corps of Engineers (USACE). (2023). National inventory of dams [Dataset]. Retrieved from <https://nid.sec.usace.army.mil/>
- United States Geological Survey (USGS). (2014). Watershed boundary dataset [Dataset]. Retrieved from <https://www.sciencebase.gov/catalog/item/51361e87e4b03b8ec4025c22>
- United States Geological Survey (USGS). (2018). National Hydrography dataset NHDPlusV2 [Dataset]. Retrieved from <https://www.epa.gov/waterdata/nhdplus-national-data>
- United States Geological Survey (USGS). (2021). National Hydrography dataset high resolution [Dataset]. Retrieved from <https://www.sciencebase.gov/catalog/item/62c6050cd34eeb1417baff15>
- United States Environmental Protection Agency (USEPA). (2007). Survey of the Nation's lakes. In *Field operations manual*. EPA841-B-07-004
- Verpoorter, C., Kutser, T., Seekell, D. A., & Tranvik, L. J. (2014). A global inventory of lakes based on high-resolution satellite imagery. *Geophysical Research Letters*, 41(18), 6396–6402. <https://doi.org/10.1002/2014gl060641>
- Wetzel, R. G. (2001). *Limnology: Lake and river ecosystems* (3rd ed.). Elsevier Academic Press.
- Yizgaw, W., Li, H. Y., Demissie, Y., Hejazi, M. I., Leung, L. R., Voisin, N., & Payn, R. (2018). A new global storage-area-depth data set for modeling reservoirs in land surface and Earth system models. *Water Resources Research*, 54(12). <https://doi.org/10.1029/2017wr022040>
- Zohary, T., & Gasith, A. (2014). The littoral zone. *Lake Kinneret: Ecology and Management*, 517–532. https://doi.org/10.1007/978-94-017-8944-8_29